Materials Science-Poland, 40(1), 2022, pp. 60-67
http://www.materialsscience.pwr.wroc.pl/
DOI: 10.2478/msp-2022-0010

sciendo

Better color distribution uniformity and higher luminous intensity for LED by using a three-layered remote phosphor structure

Nguyen Thi Phuong Loan[1], Nguyen Doan Quoc Anh[1,*], Nguyen Cong Trang[1], Hsiao-Yi Lee[2]

[1]Faculty of Electrical and Electronics Engineering, Ton Duc Thang University, Ho Chi Minh City, Vietnam
[2]Department of Electrical Engineering, National Kaohsiung University of Science and Technology, Kaohsiung, Taiwan

Angular color distribution uniformity has been one of the most relevant properties in the development of white light-emitting diodes (WLEDs), since color consistency and uniformity are crucial factors in quality evaluation of a WLED. Here, particularly considering the need to overcome the poor chromaticity usually associated with WLED, we introduce a new design for the remote-phosphor package, namely a three-layered or triple-layer (TL) phosphor structure. Using three phosphor layers in packaging a WLED can result in higher color quality and luminous efficacy, compared to the double-layer (DL) configuration. In the present study, the results of using three remote phosphor layers indicate that although the structure using three layers has a lower color rendering index, the color quality scale is better than that available from the package with two layers. Additionally, the color-deviation values in the TL structure are smaller than in the dual-layer one, especially at high color temperatures (7,700 K and 8,500 K). Besides, in comparison with the DL model, the TL package increases the luminous flux by 1.4%–2%. Therefore, the TL remote phosphor structure possesses the greatest potential in enhancing the WLED quality.

Keywords: *WLEDs, luminous efficacy, color uniformity, remote phosphor structure, three-layered remote phosphor structure*

1. Introduction

Recently, white light-emitting diodes (WLEDs) have gained much recognition among semiconductor light sources and are believed to have the potential to completely replace traditional sources of electrical illumination, such as mercury vapor, fluorescent, and high-pressure sodium lighting. Compared to these conventional lighting technologies, LED is better in energy savings, emits less heat, provides long-life performance that can be over 100,000 operating hours, and is generally associated with a lower maintenance cost [1–3]. LED lights are typically constituted by a blue-light–emitting chip coated with a thin layer of yellow-emitting phosphors and silicone compound. The blue light from LED dies passes through the phosphor layers and is partly absorbed and converted into yellow light by the yellow phosphors. This transmitted blue light and yellow light blend together to generate white light. The techniques commonly used to fabricate a LED comprise the freely dispensing and conformal phosphor-coating methods. While these methods are simple, they were found to result in a poor lumen output yield, and also, the phosphor materials became degraded quickly. The light in the dispensing and conformal coating was scattered back to the LED chip and then absorbed, causing a significant light-loss phenomenon and thus leading to poor light extraction efficiency [4, 5]. Moreover, in these traditional packaging methods, the phosphor has a direct interaction with the chip surfaces, and this increases the junction thermal generation during the operation time of an LED device, in turn lowering the performance of phosphor particles and the life span of an LED. Thus, ensuring that the phosphor coating layer is maintained at a distance from the chips can limit the generation of heat. The remote phosphor structure adapted this idea and caught the attention of researchers. This structure can reduce the proportion of light loss caused by deflection of light back to the chip, and thus improves the light

* E-mail: nguyendoanquocanh@tdtu.edu.vn

© Loan et al. 2022. This is an open access article distributed under the Creative Commons Attribution-NonCommercial-NoDerivatives 4.0 License. (http://creativecommons.org/licenses/by-nc-nd/4.0/)

transmission and extraction of LEDs [6–8]. The issue related to lumen output can be addressed with remote phosphor structure, but it cannot achieve much enhancement in color distribution uniformity [9, 10]. Further, while using a diffuser layer in the LED package decreased the energy efficiency of light transmission, this is a good method to acquire color uniformity [11–13]. Other approaches were also proposed to heighten the color properties of remote phosphor structures, such as patterned remote phosphor design [14], self-adaptive coating by slurry coating method combined with self-exposure technique [15], and single bi-color phosphor layer with red and yellow phosphor materials [16], but the luminous efficiency was somehow reduced.

The color rendering index (CRI), the currently used value to evaluate the color quality of an LED, could be enhanced by adding red phosphor into the remote phosphor layer [17]. Generally, the high CRI requires more red emission in the spectral distribution of white light, and this red-phosphor addition can provide more red-light components and achieve a higher CRI. The double-layer (DL) design for remote phosphor structure, which has a film of red-phosphor particles placed above the yellow-phosphor one, was introduced to achieve the promoted CRI. Specifically, it can obtain about 85 CRI when using red phosphor of $LiLaO_2:Eu^{3+}$ with the concentration of more than 20%; however, the luminous flux was dramatically reduced as the concentration of red phosphor increased [18]. Besides, according to the spectral power distribution (SPD) model by Gaussian function, the white light spectrum can be expressed as a tricolor spectrum of blue, green, and yellow, since the yellow phosphor $YAG:Ce^{3+}$ used in LED packages emits light in the spectrum regions of green and yellow colors [19]. Therefore, the green-phosphor layer was added to the remote phosphor structure to replace the red one. The green-yellow remote phosphor configuration can have better luminous flux but lower CRI than the red-yellow geometry [20]. Therefore, it seems difficult to simultaneously achieve color uniformity and high luminous efficacy.

In this study, our experiment involves introducing another remote phosphor structure by combining both red- and green-phosphor layers into the package. This three-layered remote phosphor configuration utilizes the red $LiLaO_2:Eu^{3+}$ and green $Zn_2GeO_4:Mn^{2+}$ phosphors. The green-phosphor layer is placed in between the yellow-phosphor and red-phosphor films. The color parameters and luminescent output of this three-layered (TL) package are calculated and examined with Mie-scattering theory and Beer's law, and then compared to those of DL structures. The obtained figures indicate that, in comparison with those of the DL model, there is a definite improvement in both the color uniformity and luminous efficiency of the TL structure. Therefore, the TL remote phosphor structure could be applied in the fabrication of a higher-quality WLED device that can provide efficient color and luminous performances.

2. Preparation

2.1. Preparing green and red phosphors

$Zn_2GeO_4:Mn^{2+}$ green-emitting phosphor is considered as a potential phosphor material for good color rendering displays. This green phosphor has green emission with a color purity of 90% and adequate intensity, while offering a good emission stability under different e-beam voltages. Besides, the red phosphor $LiLaO_2:Eu^{3+}$ showed strong photoluminescence, which was higher than those of $LaAlO_3:Eu^{3+}$ and $CsAlO_2:Eu^{3+}$, owing to its smooth surface and compact packing [21]. The peak of red light emission intensity of $LiLaO_2:Eu^{3+}$ was observed at around 620 nm, which is beneficial in terms of conserving the energy consumed corresponding to emission of red light and improving the CRI.

To successfully prepare both green- and red-phosphor layers for the modeling process and experiments, it is essential to understand the composition of each material, which is displayed in Tables 1 and 2.

The preparation of green-emitting $Zn_2GeO_4:Mn^{2+}$ phosphor can be carried out as follows: Initially, all the ingredients are well mixed in water to form a uniform slurry. The slurry is dried in air, following which it is powderized.

Table 1. The green phosphor $Zn_2GeO_4:Mn^{2+}$ composition

Ingredients	Mole (%)	By weight (g)
ZnO	90	73.2
MgF_2	5	3.1
$MnCO_3$	5	5.8
GeO_2	55	57.5

Table 2. The red phosphor $LiLaO_2:Eu^{3+}$ composition

Ingredients	Mole (%)	By weight (g)
La_2O_3	95 (of La)	155
Eu_2O_3	5 (of Eu)	8.8
Li_2CO_3	101 (of Li)	37.4

The capped quartz tubes are used to contain the powder for firing process with CO flows at 1,100°C for 1 h. Then, the product is ground or milled into powder. Subsequently, the powder is put into capped quartz tubes again and fired with water seam at 1,000°C and for 1 h. The obtained $Zn_2GeO_4:Mn^{2+}$ particles have green emission color, and a 2.31 eV emission peak is observed corresponding to the emission width of 20 eV.

To synthesize the red phosphor $LiLaO_2:Eu^{3+}$, it is important to get its chemical composition mixed evenly in methanol. Then, we let the slurry dry in air before being powderized. The powder is subsequently put into an open alumina crucible to be fired with air flows at the temperature of about 600°C. After that, this product is turned into powder. The second firing is carried out in the same container, under conditions of air, 1,000°C, and for 1 h. Once the firing for the time mentioned is completed, the following step is powderizing. Finally, the obtained powder is stored in a well-closed container. The ideal $LiLaO_2:Eu^{3+}$ particles are those that emit red light with emission peaks of 1.775–2.020 eV and have approximately a 1% e-beam excitation efficiency.

2.2. Simulation of TL remote phosphor configuration

The diagrams of WLED models are demonstrated in Figure 1 with support from the illumination design software LightTools (Synopsys, Inc., Mountain View, California). The phosphor-layer organization for two- and three-layered remote phosphor configurations is shown in Figures 1A and 1B, respectively. In particular, in the dual-layer structure, the red $LiLaO_2:Eu^{3+}$ layer is placed over the $YAG:Ce^{3+}$ yellow film. Meanwhile, in the three-layered phosphor model, the phosphor layers are in the order yellow-green-red, with yellow phosphor being the closest to the blue chip. The nine-chip package is combined with the aluminum nitride substrate and attached to the lead frame. The thickness of each phosphor film is set at 8 mm. Silicone is used to separate the phosphor layers and the chips, as represented by the blank space in the diagram shown in Figure 1. The optical performances of DL and TL structures are investigated at five correlated color temperatures (CCTs) in the range of 5,600–8,500 K.

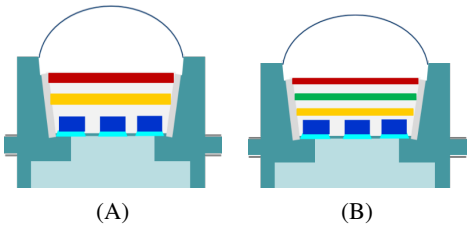


Fig. 1. Schematic diagrams of **(A)** DL remote phosphor configuration, **(B)** TL remote phosphor configuration. DL, double-layer; TL, triple-layer

The addition of two phosphor layers of green and red, apart from the original yellow one, causes a variation in the concentration of yellow phosphors. Specifically, the yellow-phosphor concentration decreases when the red or green phosphor amounts increase. This change in yellow-phosphor content has been effected so as to maintain the stability of color temperature during the operation time of LEDs. In addition, the concentration of yellow phosphor $YAG:Ce^{3+}$ at each CCT are different, and especially significantly lower at the high CCTs. Therefore, the scattering properties of lights inside the LED structure corresponding to various color temperatures are diverse, and high CCT could encourage light scattering. This also means that the optical performances of the two structures are different between CCTs.

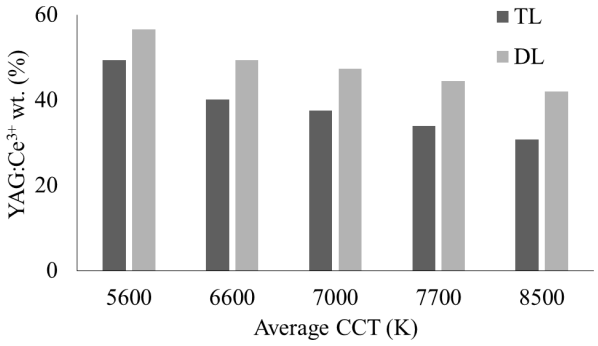


Fig. 2. Changes in yellow YAG:Ce^{3+} phosphor concentration in two remote phosphor structures at five CCTs

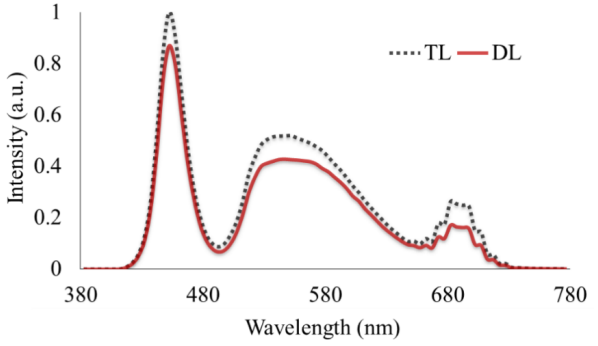


Fig. 3. Emission spectra of DL and TL phosphor structures. DL, double-layer; TL, triple-layer

In general, high yellow phosphor concentration can lead to a high proportion of backscattered light, causing increasing chances of light absorption and reducing the light extraction efficiency. As demonstrated in Figure 2, the DL configuration displays higher YAG:Ce^{3+} concentration than the TL does, at all CCTs. This may imply that the DL structure has lower luminous output (LO) than the TL package. Moreover, the high YAG:Ce^{3+} amount results in an imbalance in the chromatic distribution of yellow, red, and green light, which decreases the color uniformity of the LED package. As mentioned above, the increase in red-light emission can lead to higher color adequacy; thus, the red phosphor is utilized. Besides, the green phosphor can help to reduce backscattered light and enhance the output of luminescence. Therefore, we can surmise that the three-layered phosphor structure would be capable of simultaneously achieving better color uniformity and high luminous efficiency, since it includes both red and green phosphor films. To clarify this point, the emission spectra of both remote phosphor structures, DL and TL, should be monitored. The spectra of the DL and TL remote phosphor structures are expressed in Figure 3. It can be seen that the spectral intensities in the wavelength ranges of blue (450–480 nm), green (500–565 nm), and red (650–700 nm) of the TL are stronger than those of the DL structure. So, it is possible to improve the chromaticity performance and the lumen output intensity using the three-layered configuration.

3. Computation and discussion

The quality of a LED's chromaticity is generally examined by CRIs, which include the CRI, the most popular parameter in color evaluation. Obviously, a LED with high CRI has better brightness and a higher price. The color rendering indices of both DL and TL models at five different color temperatures are demonstrated in Figure 4. In both structures, the CRI is directly proportional to the CCT; in other words, a higher CCT has better CRI. It is noticed that the DL results in higher CRI at all CCTs. This can be attributed to the stronger red-light intensity provided by the red $LiLaO_2$:Eu^{3+} phosphor layer. Obtaining high CRI for WLEDs with high CCT is very challenging; therefore, the improvement in this color rendering ability of the

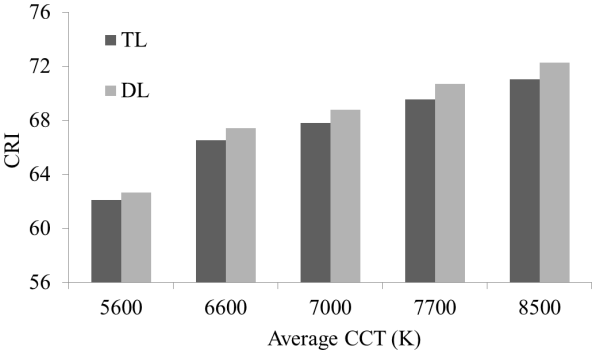


Fig. 4. CRI values of DL and TL phosphor configurations at each CCT. CRI, color rendering index; CCT, correlated color temperature; DL, double-layer; TL, triple-layer

DL and TL is noteworthy and important to the development of high-quality WLED devices. The difference between the CRI values of DL and TL structure is not too much: it is about 0.5–1; thus, either structure may be used while innovating in the attempt to carry out CRI improvements to WLEDs. However, if manufacturers aim at obtaining high CRI, it is more advantageous to apply the dual-layer structure.

CRI is an important parameter by which to measure LED brightness; yet, it does not facilitate an overall evaluation of the color quality offered by an LED device. Moreover, if the LED has an excessively high CRI or brightness, it will cause discomfort to human eyes. Therefore, the color quality scale (CQS) has emerged as an attractive parameter to researchers in examining the color quality of an LED, since it evaluates light color quality via CRI, chromatic coordinate, and observer preferences. Similar to CRI, the CQS in the DL and TL also increases with the upward movement of CCT values, as shown in Figure 5. It is obvious that the TL has better CQS than the DL, regardless of the CCT. The uniformity of chromatic distribution among the red, yellow, and green colors is observed when applying the three-layered configuration, leading to higher color performance for WLEDs. Therefore, it can be said that TL structure is appropriate for boosting the color properties of WLED packages, with excellent CQS.

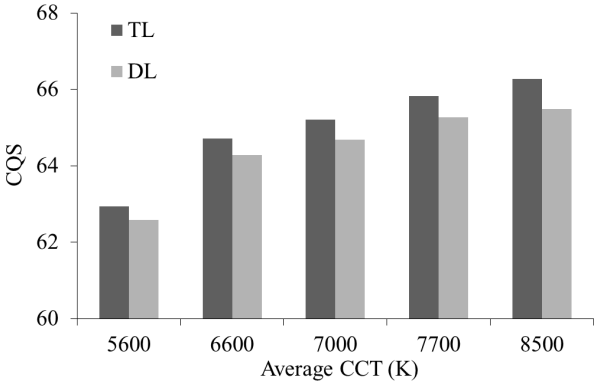


Fig. 5. CQS values of DL and TL phosphor configurations at each CCT. CQS, color quality scale; CCT, correlated color temperature; DL, double-layer; TL, triple-layer

Good color quality, or high CRI and CQS, usually leads to inefficiency in lumen output. This has raised a question as to the lumen efficiency of TL phosphor packaging, since it offers high improvement of color quality with impressive CQS results. A series of mathematic expressions pertaining to the light conversion and transmission of dual-layer and TL structures is performed based on the Mie-scattering theory to further analyze the effects of TL on LO, in comparison with the dual-layer.

The transmitted blue light and converted yellow light of DL remote phosphor with a phosphor-film thickness of h is calculated using Eqs (1) and (2), as shown below [22, 23]:

$$\begin{aligned} PB_3 &= PB_0.e^{-\alpha_{B2}\frac{2h}{3}}.e^{-\alpha_{B2}\frac{2h}{3}}.e^{-\alpha_{B2}\frac{2h}{3}} \\ &= PB_0.e^{-2\alpha_{B3}h}. \end{aligned} \tag{1}$$

$$\begin{aligned} PY_2 &= \frac{1}{2}\frac{\beta_2 PB_0}{\alpha_{B2}-\alpha_{\gamma 2}}\left[e^{-\alpha_{\gamma 2}h}-e^{-\alpha_{B2}h}\right]e^{-\alpha_{\gamma 2}h} \\ &+\frac{1}{2}\frac{\beta_2 PB_0}{\alpha_{B2}-\alpha_{\gamma 2}}\left[e^{-\alpha_{\gamma 2}h}-e^{-\alpha_{B2}h}\right] \\ &= \frac{1}{2}\frac{\beta_2 PB_0}{\alpha_{B2}-\alpha_{\gamma 2}}\left[e^{-2\alpha_{\gamma 1}h}-e^{-2\alpha_{B1}h}\right] \end{aligned} \tag{2}$$

Each phosphor layer's thickness of the TL phosphor package is demonstrated as $\frac{2h}{3}$. The computation of transmitted blue light and converted yellow light in the TL can be carried out as:

$$\begin{aligned} PB_3 &= PB_0.e^{-\alpha_{B2}\frac{2h}{3}}.e^{-\alpha_{B2}\frac{2h}{3}}.e^{-\alpha_{B2}\frac{2h}{3}} \\ &= PB_0.e^{-2\alpha_{B3}h}. \end{aligned} \tag{3}$$

$$\begin{aligned} PY'_3 &= \frac{1}{2}\frac{\beta_3 PB_0}{\alpha_{B3}-\alpha_{\gamma 3}}\left[e^{-\alpha_{\gamma 3}\frac{2h}{3}}\right. \\ &\left.-e^{-\alpha_{B3}\frac{2h}{3}}\right]e^{-\alpha_{\gamma 3}\frac{2h}{3}} \\ &+\frac{1}{2}\frac{\beta_3 PB_0 e^{-\alpha_{B3}\frac{2h}{3}}}{\alpha_{B3}-\alpha_{\gamma 3}}\left[e^{-\alpha_{\gamma 3}\frac{2h}{3}}-e^{-\alpha_{B3}\frac{2h}{3}}\right] \\ &= \frac{1}{2}\frac{\beta_3 PB_0}{\alpha_{B3}-\alpha_{\gamma 3}}\left[e^{-\alpha_{\gamma 3}\frac{4h}{3}}-e^{-2\alpha_{B3}\frac{2h}{3}}\right] \end{aligned} \tag{4}$$

$$\begin{aligned} PY_3 &= PY'_3.e^{-\alpha_{\gamma 3}\frac{2h}{3}} \\ &+PB_0.e^{-2\alpha_{B3}\frac{4h}{3}}\frac{1}{2}\frac{\beta_3}{\alpha_{B3}-\alpha_{\gamma 3}}\left[e^{-\alpha_{\gamma 3}\frac{2h}{3}}-e^{-\alpha_{B3}\frac{2h}{3}}\right] \end{aligned} \tag{5}$$

$$= \frac{1}{2}\frac{\beta_3 PB_0}{\alpha_{B3}-\alpha_{\gamma 3}}\left[e^{-\alpha_{\gamma 3}\frac{4h}{3}} - e^{-\alpha_{B3}\frac{4h}{3}}\right]e^{-\alpha_{\gamma 3}\frac{2h}{3}}$$
$$+ \frac{1}{2}\frac{\beta_3 PB_0 e^{-\alpha_{B3}\frac{4h}{3}}}{\alpha_{B3}-\alpha_{\gamma 3}}\left[e^{-\alpha_{\gamma 3}\frac{2h}{3}} - e^{-\alpha_{B3}\frac{2h}{3}}\right]$$
$$= \frac{1}{2}\frac{\beta_3 PB_0}{\alpha_{B3}-\alpha_{\gamma 3}}\left[e^{-\alpha_{\gamma 3}h} - e^{-2\alpha_{B3}h}\right]$$

where h shows the thickness of each phosphor layer in both DL and TL structures; the subscripted *"2"* and *"3"* indicate the DL and TL structures, respectively; β presents the conversion coefficient of blue light transformed to yellow light in the package; γ shows the yellow-light reflection coefficient; PB presents blue-light intensity and PY indicates yellow-light intensity; PB_0 is the LED-die emitted light intensity comprised of PB and PY; PY'_3 is the intensity of the yellow light transmitted through both red- and green-phosphor layers; and α_B and α_Y indicate the fractions of blue-light and yellow-light energy loss, respectively.

The TL structure improves the lighting output of LEDs, and renders it significantly better than the results obtained from the dual-layer configuration, as can be observed in Eq. (6):

$$\frac{(PB_3 - PY_3) - (PB_2 + PY_2)}{(PB_2 + PY_2)} > \frac{e^{-2\alpha_{B3}h} - e^{-2\alpha_{B2}h}}{e^{-2\alpha_{\gamma 3}h} - e^{-2\alpha_{B2}h}} > \tag{6}$$

As mentioned, Mie-theory [24, 25] is applied in the scattering analysis of phosphor materials and in determining the scattering cross-section C_{sca}. The power of transmitted light is calculated based on Beer's law:

$$I = I_0 \exp(-\mu_{ext} L) \tag{7}$$

Here, I_0 shows the power of incident light, and L and μ_{ext} demonstrate the thickness of each phosphor layer and the extinction coefficient, respectively. Besides, the calculation of the extinction coefficient is: $\mu_{ext} = N_r.C_{ext}$. In this formula, N_r indicates the particles' density distribution number (mm^{-3}), and C_{ext} (mm^2) presents the extinction cross-section phosphor spheres.

The effectiveness of using TL structure to improve the luminous flux can be inferred from Eq. (6). The lumen outputs of the DL and TL configurations are also expressed in Figure 6, from which we infer that the TL achieves about 2% enhancement in luminescence, compared to that achieved using the DL. Particularly, the luminous flux of the TL and DL increase when the CCT becomes higher. The superior lumen output of the TL in comparison with that of the DL can be observed clearly at high CCTs such as 7,700 K and 8,500 K. These impressive luminescence results in the TL model can be attributed to the higher green light emission when using the green phosphor Zn_2GeO_4:Mn^{2+}, which is much greater than that from the DL, owing to the degradation of yellow-phosphor concentration for maintaining the stability of color temperature. This means the TL can reduce the backscattering and reabsorption of light, which enhances the efficiency of blue light transmission through the yellow-phosphor layers, facilitating the former to be converted effectively. It is also pointed out in Figure 3 that the TL results in higher red-light emission, thus resulting in greater enhancement in the color quality. Thus, the TL can yield high LO and enhance the chromaticity of LED at the same time.

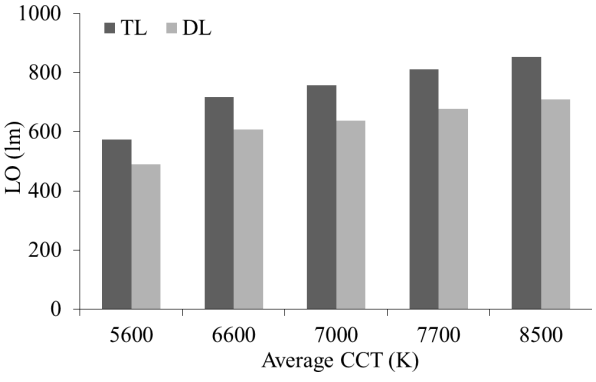


Fig. 6. Luminous output (LO)

The angular chroma variation (D-CCT) of a LED package also plays an important role in light-chromaticity evaluation. The smaller the D-CCT presented, the more the chromatic homogeneity is improved. Accordingly, the results of D-CCT in the TL and the DL remote models are analyzed and presented in Figure 7. The color variations in the TL are much lower than in the DL. As can be

seen, the D-CCT corresponding with the CCTs of TL is about 200–2,000 K smaller than that of the DL, which indicates the effectiveness of the TL in achieving higher chromatic homogeneity. This can result from the increase in the scattering properties of light when there are more phosphor layers in the remote structure. The improvement in light scattering probably leads to better light color mixing and distribution, and thus results in a reduction of the color variations. Yet, one disadvantage of scattering improvement is that it decreases the luminescence. However, the TL presents higher lumen output, better CQS, and significant reduction in backscattering events; therefore, a small decrease in its lumen intensity can be accepted.

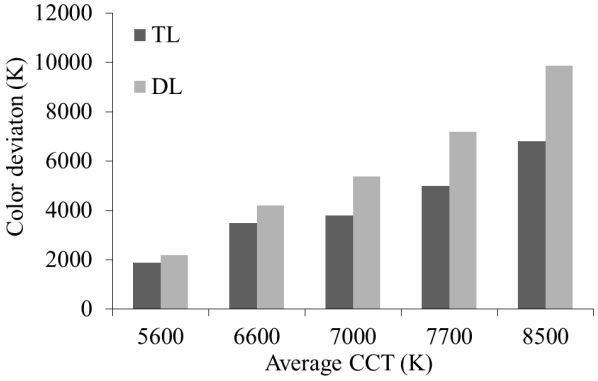


Fig. 7. Color deviation (D-CCT) of TL and DL phosphor configurations at each CCT. CCT, correlated color temperature. DL, double-layer; TL, triple-layer

4. Conclusions

The effectiveness of the three-layered or TL remote phosphor configuration is demonstrated in this study. The green phosphor Zn_2GeO_4:Mn^{2+} and red phosphor $LiLaO_2$:Eu^{3+} are utilized for the model fabrication. Although the TL structure has a lower CRI, its CQS performs better since the color imbalance among red, yellow, and green is addressed. Also, the LO of the TL is higher than that of the DL due to the stronger green emission in the spectral region. The greater number of phosphor layers included in the TL structure enhances the scattering ability, which induces a reduction in backscattering, in turn leading to heightened blue-light transmission and conversion. The scattering improvement also increases the light color blending and results in a more uniform color distribution, thus lessening the color deviations. Though the higher scattering properties can cause a decrease in the lumen intensity, the benefits that the TL structure brings to the optical performance of LEDs via backscattering reduction have outweighed this drawback. Therefore, manufactures can apply the three-layered remote phosphor structure to accomplish higher-quality LED packages.

References

[1] Luo GF, Loan NTP, Tho LV, Anh NDQ, Lee HY. Enhancement of color quality and luminous flux for remote-phosphor LEDs with red-emitting $CaMgSi_2O_6$:Eu^{2+}, Mn^{2+}. Mater Sci-Pol. 2020;38:409–15.

[2] Anh NDQ, Ngoc HV. Building superior lighting properties for WLEDs utilizing two-layered remote phosphor configurations. Mater Sci-Pol. 2020;38:493–501.

[3] Yen WM, Weber MJ. Inorganic phosphors: compositions, preparation and optical properties. Boca Raton, Florida: CRC Press; 2004. p. 33431.

[4] Davis W, Ohno Y. Color quality scale. Opt Eng. 2010;49:033602–16.

[5] Liu ZY, Liu S, Wang K, Luo XB. Measurement and numerical studies of optical properties of YAG:Ce phosphor for white light-emitting diode packaging. Appl Opt. 2010;49:247–57.

[6] Zhang GZ, Ding K, He GX, Zhong P. Spectral optimization of color temperature tunable white LEDs with red LEDs instead of phosphor for an excellent IES color fidelity index. OSA Continuum. 2019;2:1056–64.

[7] Liu X, Lei RS, Huang FF, Deng DG, Wang HP, Zhao SL, et al. Upconversion luminescence, intrinsic optical bistability, and optical thermometry in Ho^{3+}/Yb^{3+}: $BaMoO_4$ phosphors. Chin Opt Lett. 2019:17;111–601.

[8] Yang X, Chai CF, Chen JC, Zheng SS, Chen C. Single 395 nm excitation warm WLED with a luminous efficiency of 104.86 lm/W and a color rendering index of 90.7. Opt Mater Express. 2019;9:4273–86.

[9] Li LP, Qin F, Zhou Y, Zhang XY, Li L, Gao H, et al. "Roller coaster"-like thermal evolution of the Er3+ ion's red photoluminescence in CaWO4:Yb3+/Er3+ phosphors. Opt Lett. 2019;44:4411–4.

[10] Tian C, Lin H, Zhang DW, Zhang PP, Hong RJ, Han ZX, et al. Mn^{4+} activated Al_2O_3 red-emitting ceramic phosphor with excellent thermal conductivity. Opt Express. 2019;27:32666–78.

[11] Zhang ZJ, Yang WC. Tunable photoluminescence in Ba1-xSrx$Si_3O_4N_2$:Eu^{2+}/Ce^{3+}, Li^{+} solid solution phosphors induced by linear structural evolution. Opt Mater

Express. 2019;9:1922–32.

[12] Wei T, Bo W, Yan C, Yeqing C, Jun L, Qingguang Z. Single Pr3+-activated high-color-stability fluoride white-light phosphor for white-light-emitting diodes. Opt Mater Express. 2019;9:223–33.

[13] Lin D, Ho W, Chen G, Liu J, Pan B, Haung Y, et al. Silicon solar cells efficiency enhanced in NIR band by coating plasmonics ITO- and UC phosphors-particles layers on back-side surface using spin-on film deposition. In: Conference on lasers and electro-optics, OSA technical digest. Optical Society of America; 2019. Paper ATh1I.4.

[14] Wang B, Li DS, Shen LF, Pun EYB, Lin H. Eu^{3+} doped high-brightness fluorophosphate laser-driven glass phosphors. Opt Mater Express. 2019;9:1749–62.

[15] Chen J, Tang YR, Yi XZ, Tian YN, Ao G, Hao DM, et al. Fabrication of $(Tb,Gd)_3Al_5O_{12}:Ce^{3+}$ phosphor ceramics for warm white light-emitting diodes application. Opt Mater Express. 2019;9:3333–41.

[16] Chen FB, Chi KL, Yen WY, Sheu JK, Lee ML, Shi JW. Investigation on modulation speed of photon-recycling white light-emitting diodes with vertical-conduction structure. J Lightwave Technol. 2019;37:1225–30.

[17] Fuertes V, Fernández JF, Enríquez E. Enhanced luminescence in rare-earth-free fast-sintering glass-ceramic. Optica. 2019;6:668–79.

[18] Wan RG, Zhang S, Liu ZQ, Yi XY, Wang LC, Wang JX, et al. Simultaneously improve the luminous efficiency and color-rendering index of GaN-based white-light-emitting diodes using metal localized surface plasmon resonance. Opt Lett. 2019;44:4155–8.

[19] Huang XY, Wang SY, Li B, Sun Q, Guo H. High-brightness and high-color purity red-emitting $Ca_3Lu(AlO)_3(BO_3)_4:Eu^{3+}$ phosphors with internal quantum efficiency close to unity for near-ultraviolet-based white-light-emitting diodes. Opt Lett. 2018;43:1307–10.

[20] Lu DS, Gong XH, Chen YJ, Huang JH, Lin YF, Luo ZD, et al. Synthesis and photoluminescence characteristics of the $LiGd_3(MoO_4)^5:Eu^{3+}$ red phosphor with high color purity and brightness. Opt Mater Express. 2018;8;259–69.

[21] Peng Y, Mou Y, Guo X, Xu XJ, Li H, Chen MX, et al. Flexible fabrication of a patterned red phosphor layer on a $YAG:Ce^{3+}$ phosphor-in-glass for high-power WLEDs. Opt Mater Express. 2018;8:605–14.

[22] Ding XR, Chen Q, Tang Y, Li JS, Talwar DP, Yu BH, et al. Improving the optical performance of multi-chip LEDs by using patterned phosphor configurations. Opt Express. 2018;26:A283–92.

[23] Zhou ZZ, Liu GG, Ni J, Liu WL, Liu Q. White light obtainment via tricolor luminescent centers and energy transfer in $Ca_3ZrSi_2O_9:Eu^{3+}$, Bi^{3+}, Tb^{3+} phosphors. Opt Mater Express. 2018;8:3526–42.

[24] Li XP, Zhong H, Chen BJ, Sui GZ, Sun JS, Xu S, et al. Highly stable and tunable white luminescence from Ag-Eu^{3+} co-doped fluoroborate glass phosphors combined with violet LED. Opt Express. 2018;26:1870–81.

[25] Chen MJ, Loan NTP, Tho LV, Minh BT, Le PX, Quoc Anh ND, et al. The impacts of $Ba_2Li_2Si_2O_7:Sn^{2+}$, Mn^{2+} and $CaMgSi_2O_6:Eu^{2+}$, Mn^{2+} particles on the optical properties of remote phosphor LED. Mater Sci-Pol. 2020;38:197–205.

Received 2021-05-19
Accepted 2021-09-23